GENERALIZED ENERGY CONDENSATION THEORY

A Thesis
Presented to
The Academic Faculty

by

Steven James Douglass

In Partial Fulfillment
of the Requirements for the Degree
Master of Science in Nuclear Engineering

Georgia Institute of Technology
December 2007

GENERALIZED ENERGY CONDENSATION THEORY

Approved by:

Dr. Farzad Rahnema, Advisor
School of Mechanical Engineering
Georgia Institute of Technology

Dr. Weston Stacey
School of Mechanical Engineering
Georgia Institute of Technology

Dr. Ronaldo Szilard
Director of Nuclear Science and Engineering
Idaho National Laboratory

Date Approved: November 8, 2007

ACKNOWLEDGEMENTS

I would first like to thank Dr. Rahnema, whose guidance, motivation, and tireless patience has been invaluable in the last couple of years. I would also like to thank Dingkang Zhang, for offering valuable insight in helping develop this work, as well as Dr. Stacey and Dr. Szilard, for serving on my reading committee.

I would like to thank my parents, who have always been supportive of my educational efforts, and who have always been willing to help me in any way I need for as long as I have lived. I could not have achieved anything without the foundation upon which I was raised.

Lastly, I would like to thank my brothers. They have been a constant source of encouragement in my graduate endeavors, and without them, I would likely not have gone to graduate school at Georgia Tech.

TABLE OF CONTENTS

LIST OF TABLES

LIST OF FIGURES

SUMMARY

A generalization of multigroup energy condensation theory has been developed. The new method generates a solution within the few-group framework which exhibits the energy spectrum characteristic of a many-group transport solution, without the computational time usually associated with such solutions. This is accomplished by expanding the energy dependence of the angular flux in a set of general orthogonal functions. The expansion leads to a set of equations for the angular flux moments in the few-group framework. The 0^{th} moment generates the standard few-group equation while the higher moment equations generate the detailed spectral resolution within the few-group structure.

It is shown that by carefully choosing the orthogonal function set (e.g., Legendre polynomials), the higher moment equations are only coupled to the 0^{th}-order equation and not to each other. The decoupling makes the new method highly competitive with the standard few-group method since the computation time associated with determining the higher moments become negligible as a result of the decoupling. The method is verified in several 1-D benchmark problems typical of BWR configurations with mild to high heterogeneity.

CHAPTER 1

INTRODUCTION

Multigroup treatment of the energy variable is extensively used in solving the transport equation or its diffusion approximation in reactor physics problems. For solving fixed source or eigenvalue problems in large complicated systems such as reactors, it is common practice, for the sake of efficiency and practicality, to condense the cross section data from an ultra-fine-group format to a set that is manageable (e.g., fine or coarse group) in terms of computational resource (memory and time) limitation and the desired accuracy. The condensation procedure requires the exact energy spectrum of the flux as a weighting function, which is not known a priori. As a result, approximate flux spectra are obtained for smaller subregions of the system (e.g., lattice cell) with approximate boundary conditions (e.g., full specular reflection), which are used to condense the cross sections into a smaller number of groups. Clearly, this condensation procedure results in loss of energy resolution in addition to accuracy.

Recovering the energy resolution while maintaining the computational efficiency is highly desirable in both eigenvalue (criticality) and fixed source (shielding) calculations. In this paper, we develop a new method to recover (unfold) the energy spectrum to any desired resolution (e.g., from coarse to fine or ultra-fine, fine to ultra-fine). This is achieved by generalizing the standard condensation procedure, assuming that the energy dependence of the neutron flux (spectrum) may be expanded in a set of orthogonal basis functions, and folding this dependence into the cross section condensation process. It will be shown that the standard condensation procedure is

contained within this generalized method as a 0^{th}-order approximation, and that through implementing this method, the computation time is reduced to that of standard coarse-group computations, but with the detail usually associated with much finer group solutions. The validity of the new method will be demonstrated by application to several one-dimensional problems with varying degrees of heterogeneity. The method is derived and tested in transport theory. Its extension to its diffusion approximation is straightforward.

CHAPTER 2

BACKGROUND

Methods for treating the energy dependence of the neutron flux in a reactor are many and varied. The usual multi-group formulation with few-group condensation is by far the most common, but a great deal of work has been done to find improved methods for treating the energy spectrum. Work by M. L. Williams and M. Asgari [1] formulated a combination of multi-group theory and continuous-energy theory to improve the calculation of the energy spectrum in the resonance region. Their work takes advantage of a Legendre "Sub-moment Expansion" in the scattering transfer function, and breaks the energy spectrum into three regions, using multi-group theory in the fast and thermal ranges, and a point-wise solution in the resonance region, all within a one-dimensional discrete-ordinates framework.

Work has also been done in reactor analysis using point-wise energy lattice methods. M. L. Zerkle has developed methods for solving the neutron transport equation using a near-continuous energy point-wise solution method which collapses the energy dependence to a small number of groups from point-wise data [2,3]. These methods have been applied in the RAZOR lattice code by Zerkle, Abu-Shumays, Ott, and Winwood. Work by M. L. Williams has also provided a solution for thermal neutrons in a reactor using continuous energy methodology implemented in the CENTRM solution module for the SCALE code system [4]. These techniques were all developed to improve the resonance and energy treatments within the multi-group methodology.

Most work focusing on energy dependence has thus far been towards improving the accuracy of the multigroup approximation to the solution within single assemblies. There has not been much work towards preserving the spectral information during the condensation procedure and whole core calculation, where the detailed spectrum information is lost. Work by Silver, Roeder, Voter, and Kress addresses a method of Kernel Polynomial Approximation for spectral functions, using applications of polynomial expansion in the computation of the density of energy states within electronic structures [5]. This allows for treatment of spectral functions with polynomial expansions in a straightforward and accurate way. Their work fully treats the method for Chebyshev Polynomials, and it has similar applications to work that can be used in nuclear reactor computations, particularly in the treatment of the angular dependence of the scattering kernel.

CHAPTER 3

METHOD

The generalized energy condensation theory represents a method whereby the energy spectrum of the neutron flux is produced to a high degree of accuracy during a few-group calculation. This method begins by generating fine-group cross sections, as well as a fine-group transport solution for the individual lattice cells (e.g., fuel assemblies) which make up the system. The method of fine-group cross section generation is entirely independent of the generalized theory, and should be done in whatever manner the user deems appropriate. For example, lattice depletion codes generate fine or ultra-fine-group cross sections by properly accounting for resonance smearing and temperature effects. Similarly, fine or ultra-fine-group transport solutions within each assembly may be obtained using any computational method appropriate for the desired application (e.g., discrete ordinates, collision probability, etc). In addition, the method is independent of the treatment of the angular dependence of the scattering kernel, and the user may use any desired technique.

The fine-group transport solution within each lattice cell (fuel assembly) is then used as a weighting function in the generation of orthogonal expansion moments for the energy dependence of the cross sections and reaction rates for each region of the assembly for a set of coarse-groups. This replaces the standard condensation procedure, which uses the ultra-fine or fine-group transport solution to generate fine or coarse-group cross sections that are constant in energy within each coarse group. Using the expansion moments of the cross sections and reaction rates, the problem is then solved via a coupled

set of modified transport equations for the whole core. The resultant series of flux moments within each coarse-group can then be used to construct the fine group energy spectrum of the neutron distribution in the entire core. The core energy spectrum is not accessible using the current standard condensation methods, but obtained using the generalized method presented here.

The generalized method is entirely independent of the transport solution methodology (e.g., spatial differencing and angular approximation schemes), and therefore allows for a high degree of flexibility in application. It expands the standard few-group equations into a new set of expansion equations, which are then solved in any manner desired. The standard condensation method is a special case (the 0^{th} order) of the general theory. The additional moment equations coupled to the 0^{th} order represent correction terms to the energetically flat flux assumed in the standard few-group model. It is noted that with a properly chosen expansion basis, this method can be used to generate very high order expansions with negligible computation time due to the decoupling of the set of equations, to be described in a later section.

The new method is tested by considering some 1-D example problems. Legendre polynomials are used as the basis function and the lattice depletion code HELIOS [8] is used to generate the fine-group cross sections in these examples. Fine-group transport solutions, which are generated using a discrete-ordinates code written for the purpose of testing the new method, are then used as the weighting function for the generation of expansion moments.

3.1 Derivation

Within a reactor of arbitrary geometry, the balance of neutrons at position $\vec{r}$ with lethargy *u* and moving in a direction $\hat{\Omega}(\theta,\varphi)$ is described by the transport equation in its integro-differential form (Eq. (1)).

$$\hat{\Omega}\cdot\nabla\psi(\vec{r},\hat{\Omega},u)+\sigma(\vec{r},u)\psi(\vec{r},\hat{\Omega},u)=\int_0^\infty du'\int_{4\pi}d\hat{\Omega}'\sigma_s(\vec{r},\hat{\Omega}'\to\hat{\Omega},u'\to u)\psi(\vec{r},\hat{\Omega}',u') + \frac{\chi(u)}{k}\int_0^\infty du'\int_{4\pi}d\hat{\Omega}'\nu\sigma_f(\vec{r},u')\psi(\vec{r},\hat{\Omega}',u') \tag{1}$$

where $\Psi(\vec{r},u,\hat{\Omega})$ is the angular flux and $\sigma(\vec{r},u)$ represents the total macroscopic reaction cross section at position $\vec{r}$ for neutrons with lethargy *u*. The function $\sigma_s(\vec{r},\hat{\Omega}'\to\hat{\Omega},u'\to u)$ is the macroscopic scattering cross section at position $\vec{r}$ with incoming lethargy u' and angle $\hat{\Omega}'$ and outgoing lethargy *u* and angle $\hat{\Omega}$. The system multiplication constant is represented by *k* and $\nu\sigma_f(\vec{r},u')$ and $\chi(u)$ are the fission neutron production cross section and fission spectrum, respectively.

The lethargy integrals on the right hand side of Eq. (1) can be broken up into smaller regions representing the energy intervals of the few-group structure chosen. (The number of few-groups G is arbitrary.) By applying the segmentation to the lethargy integral terms in Eq. (1) and breaking the spectrum into G (coarse) groups, Eq. (1) becomes

$$\hat{\Omega}\cdot\nabla\psi(\vec{r},\hat{\Omega},u)+\sigma(\vec{r},u)\psi(\vec{r},\hat{\Omega},u)=\sum_{g=0}^{G-1}\int_{\Delta u_g}du'\int_{4\pi}d\hat{\Omega}'\sigma_s(\vec{r},\hat{\Omega}'\to\hat{\Omega},u'\to u)\psi(\vec{r},\hat{\Omega}',u') + \sum_{g=0}^{G-1}\frac{\chi(u)}{k}\int_{\Delta u_g}du'\int_{4\pi}d\hat{\Omega}'\nu\sigma_f(\vec{r},u')\psi(\vec{r},\hat{\Omega}',u') \tag{2}$$

where Δu_g is the lethargy interval of coarse-group *g*. The infinite-lethargy bound on the integral in Eq. (1) has also been chosen to be some value large enough to admit few neutrons beyond it.

In the example problems presented later, the upper lethargy limit is chosen to be 26.022, corresponding to an energy of 0.0001 eV. This value was chosen to correspond to the energy bounds of the 47-group cross sections obtained from the lattice depletion code HELIOS, and could be changed to fit other applications, such as radiation detection or shielding problems.

As has been previously mentioned, the angular dependence of the scattering kernel can be treated in its most general form. For the derivations that follow, the angular dependence of the scattering kernel is treated with an expansion in angle using Spherical Harmonics [6], and fission is treated as isotropic:

$$\hat{\Omega}\cdot\nabla\psi(\vec{r},\hat{\Omega},u)+\sigma(\vec{r},u)\psi(\vec{r},\hat{\Omega},u)=\sum_{g=0}^{G-1}\sum_{l=0}^{\infty}\sum_{m=-1}^{1}\frac{Y_{lm}^{*}(\hat{\Omega})}{4\pi}\int_{\Delta u_g}du'\sigma_{sl}(\vec{r},u'\rightarrow u)\phi_l^m(\vec{r},u') + \sum_{g=0}^{G-1}\frac{\chi(u)}{4\pi k}\int_{\Delta u_g}du'\nu\sigma_f(\vec{r},u')\phi(\vec{r},u') \tag{3}$$

where $\phi(\vec{r},u')$ is the scalar flux at position $\vec{r}$ and lethargy u', and $\sigma_{sl}(\vec{r},u'\rightarrow u)$ and $\phi_l^m(\vec{r},u')$ represent angular moments of the scattering kernel and angular flux:

$$\sigma_{sl}(\vec{r},u'\rightarrow u)=\frac{1}{2}\int_{-1}^{1}d\mu_o\sigma_s(\vec{r},u'\rightarrow u,\mu_o)P_l(\mu_o) \tag{4}$$

$$\phi_l^m(\vec{r},u')=\int_{4\pi}d\hat{\Omega}'Y_{lm}(\hat{\Omega}')\Psi(\vec{r},u',\hat{\Omega}') \tag{5}$$

where $Y_{lm}(\hat{\Omega})$ are the normalized spherical harmonics, and $\mu_o=\hat{\Omega}\cdot\hat{\Omega}'$ is the cosine of the scattering angle. The function $P_l(\mu)$ represents the l^{th} order Legendre polynomials.

In order to expand the angular flux in a particular lethargy region, we must first ensure that the basis functions chosen are orthogonal over it. Since this is to be done for an arbitrary set of orthogonal basis functions, the lethargy variable is changed to a scaled variable within each group to align the interval of that group with the interval of orthogonality for the basis set. Therefore, a new variable is defined in each group:

$$u_g = \left(\frac{u - u_i}{u_f - u_i} \right) \Delta u_\perp + u_{i\perp} \tag{6}$$

where u_i and u_f are the bounds of $\Delta u_g = u_f - u_i$, the lethargy interval of the coarse-group, and $u_{i\perp}$ and $u_{f\perp}$ are the bounds of $\Delta u_\perp = u_{f\perp} - u_{i\perp}$, the interval of orthogonality of the basis functions. To preserve the neutron distribution under this transformation, we enforce the balance conditions

$$\Psi(\vec{r},u,\hat{\Omega})du = \Psi(\vec{r},u_g,\hat{\Omega})du_g \quad \text{and} \quad \sigma_x(\vec{r},u) = \sigma_x(\vec{r},u_g) \tag{7}$$

where $\sigma_x(\vec{r},u)$ represents the cross sections of the system. This allows the right hand side (*RHS*) of Eq. (3) to be written as:

$$RHS = \sum_{g=0}^{G-1} \sum_{l=0}^{\infty} \sum_{m=-1}^{1} \frac{Y_{lm}^*(\hat{\Omega})}{4\pi} \int_{\Delta u_\perp} du_g' \sigma_{sl}(\vec{r},u_g' \to u) \phi_l^m(\vec{r},u_g') + \sum_{g=0}^{G-1} \frac{\chi(\vec{r},u)}{4\pi k} \int_{\Delta u_\perp} du_g' \nu\sigma_f(\vec{r},u_g') \phi(\vec{r},u_g') \tag{8}$$

As a consequence of the balance condition above, the following transformations result:

$$\Psi(\vec{r},u,\hat{\Omega}) = \Psi(\vec{r},u_h,\hat{\Omega}) \frac{\Delta u_\perp}{\Delta u_h}, \quad \chi(\vec{r},u) = \chi(\vec{r},u_h) \frac{\Delta u_\perp}{\Delta u_h}, \quad \sigma_{sl}(\vec{r},u_g' \to u) = \sigma_{sl}(\vec{r},u_g' \to u_h) \frac{\Delta u_\perp}{\Delta u_h} \tag{9}$$

With the assumption that the transport equation is valid for all values of the lethargy *u*, Eq. (3) can be split into G coupled equations, each describing the neutron balance within its own group *h*, with the lethargy variable scaled using the above transformations.

Therefore, neutron balance within a coarse-group *h*, with lethargy u_h, position $\vec{r}$, and direction $\hat{\Omega}$ is given by Eq. (10).

$$\begin{aligned}\hat{\Omega}\cdot\nabla\psi(\vec{r},\hat{\Omega},u_h)+\sigma(\vec{r},u_h)\psi(\vec{r},\hat{\Omega},u_h)=&\sum_{g=0}^{G-1}\sum_{l=0}^{\infty}\sum_{m=-1}^{1}\frac{Y_{lm}^{*}(\hat{\Omega})}{4\pi}\int_{\Delta u_\perp}du_g'\sigma_{sl}(\vec{r},u_g'\to u_h)\phi_l^m(\vec{r},u_g')\\&+\sum_{g=0}^{G-1}\frac{\chi(\vec{r},u_h)}{4\pi k}\int_{\Delta u_\perp}du_g'\nu\sigma_f(\vec{r},u_g')\phi(\vec{r},u_g')\end{aligned}\tag{10}$$

3.1.1 Orthogonal Expansion

Assume a set of orthogonal functions of lethargy within coarse-group *h:* $\xi_i(u_h)$, which obey the orthogonality condition on $\Delta u_\perp$:

$$\int_{\Delta u_\perp}du_h w(u_h)\xi_i(u_h)\xi_j(u_h)=\frac{\delta_{ij}}{\alpha_j}\tag{11}$$

where $w(u_h)$ is a weighting function, δ_{ij} is the Kronecker Delta, and α_j is a normalization constant determined by the choice of $\xi_i(u_h)$. Any function $f(u_h)$ on $\Delta u_\perp$ can be then written according to the expansion:

$$f(u_h)=\sum_{i=0}^{\infty}\alpha_i f_i\xi_i(u_h)\quad\text{where}\quad f_i=\int_{\Delta u_\perp}du_h f(u_h)w(u_h)\xi_i(u_h).\tag{12}$$

Multiplying Eq. (10) by $w(u_h)\,\xi_i(u_h)$ and integrating over the orthogonality limits, which represent the lethargy bounds of group *h*, one obtains:

$$\begin{aligned}&\hat{\Omega}\cdot\nabla\Psi_{ih}(\vec{r},\hat{\Omega})+\sigma_{ih}(\vec{r},\hat{\Omega})\Psi_{ih}(\vec{r},\hat{\Omega})\\&\quad=\sum_{g=0}^{G-1}\sum_{l=0}^{\infty}\sum_{m=-1}^{1}\frac{Y_{lm}^{*}(\hat{\Omega})}{4\pi}\int_{\Delta u_\perp}du_h w(u_h)\xi_i(u_h)\int_{\Delta u_\perp}du_g'\sigma_{sl}(\vec{r},u_g'\to u_h)\phi_l^m(\vec{r},u_g')\\&\qquad+\sum_{g=0}^{G-1}\frac{\chi_{ih}(\vec{r})}{4\pi k}\int_{\Delta u_\perp}du_g'\nu\sigma_f(\vec{r},u_g')\phi(\vec{r},u_g')\end{aligned}\tag{13}$$

where the following energy (lethargy) moments have been introduced:

$$\Psi_{ih}(\vec{r},\hat{\Omega}) = \int_{\Delta u_\perp} du_h \Psi(\vec{r},\hat{\Omega},u_h) w(u_h) \xi_i(u_h) \tag{14}$$

$$\sigma_{ih}(\vec{r},\hat{\Omega}) = \frac{\int_{\Delta u_\perp} du_h \sigma(\vec{r},u_h)\Psi(\vec{r},\hat{\Omega},u_h) w(u_h) \xi_i(u_h)}{\int_{\Delta u_\perp} du_h \Psi(\vec{r},\hat{\Omega},u_h) w(u_h) \xi_i(u_h)} \tag{15}$$

$$\chi_{ih}(\vec{r},\hat{\Omega}) = \int_{\Delta u_\perp} du_h \chi(\vec{r},\hat{\Omega},u_h) w(u_h) \xi_i(u_h) \tag{16}$$

The moments $\sigma_{ih}(\vec{r},\hat{\Omega})$ and $\chi_{ih}(\vec{r},\hat{\Omega})$ are computed numerically, with $\sigma_{ih}(\vec{r},\hat{\Omega})$ weighted with the flux distribution obtained in a fine-group calculation (e.g., for a single assembly).

The collision term is modified to expand not the total reaction rate, as in Eq. (15), but rather to expand the deviation of the total collision reaction rate from the mean within each group, based on standard perturbation techniques. Thus, the total cross section within group *h* is rewritten as:

$$\sigma(\vec{r},u,\hat{\Omega}) = \sigma_{0h}(\vec{r},\hat{\Omega}) + \delta(\vec{r},u,\hat{\Omega}) \tag{17}$$

where $\delta(\vec{r},u,\hat{\Omega})$ is the perturbation of the cross section from the spectral mean, and $\sigma_{0h}(\vec{r},\hat{\Omega})$ is the standard form of the flux-weighted cross-section in coarse group *h*, as defined in Eq. (18).

$$\sigma_{0h}(\vec{r},\hat{\Omega}) = \frac{\int_{\Delta u_\perp} du_h \sigma(\vec{r},u_h)\Psi(\vec{r},\hat{\Omega},u_h)}{\int_{\Delta u_\perp} du_h \Psi(\vec{r},\hat{\Omega},u_h)} \tag{18}$$

Thus, when multiplying Eq. (10) by $w(u_h)\ \xi_i(u_h)$ and integrating, as done before, the collision term changes, and Eq. (13) becomes:

$$\begin{aligned}\hat{\Omega}\cdot\nabla\Psi_{ih}(\vec{r},\hat{\Omega})+\sigma_{0h}(\vec{r},\hat{\Omega})\Psi_{ih}(\vec{r},\hat{\Omega})+\delta_{ih}(\vec{r},\hat{\Omega})\Psi_{0h}(\vec{r},\hat{\Omega})\\ =\sum_{g=0}^{G-1}\sum_{l=0}^{\infty}\sum_{m=-1}^{1}\frac{Y_{lm}^{*}(\hat{\Omega})}{4\pi}\int_{\Delta u_\perp}du_h w(u_h)\xi_i(u_h)\int_{\Delta u_\perp}du_g'\sigma_{sl}(\vec{r},u_g'\to u_h)\phi_l^m(\vec{r},u_g')\\ +\sum_{g=0}^{G-1}\frac{\chi_{ih}(\vec{r})}{4\pi k}\int_{\Delta u_\perp}du_g'\nu\sigma_f(\vec{r},u_g')\phi(\vec{r},u_g')\end{aligned}\tag{19}$$

where the moment of the total cross-section perturbation is defined as

$$\delta_{ih}(\vec{r},\hat{\Omega})=\frac{\int_{\Delta u_\perp}du_h\delta(\vec{r},u_h)\Psi(\vec{r},\hat{\Omega},u_h)w(u_h)\xi_i(u_h)}{\int_{\Delta u_\perp}du_h\Psi(\vec{r},\hat{\Omega},u_h)w(u_h)\xi_0(u_h)}\tag{20}$$

In this manner, the only moment in the denominator of the perturbation is the 0th-order flux moment, which is typically the largest, and therefore least likely to be too small. This technique greatly reduces the likelihood of numerical issues due to dividing by near-zero flux moments.

Treating the energy dependence of the right hand side of Eq. (13) is complicated by the desire to ensure that the total neutron reaction rates on the right hand side are preserved for expansions of arbitrary order. To ensure that this is the case, rather than condensing the cross sections directly, the reaction rate energy density is expanded in orthogonal functions. Let

$$\Re_f(\vec{r},u_g')=\nu\sigma_f(\vec{r},u_g')\phi(\vec{r},u_g')\tag{21}$$

$$\Re_{s,l}^m(\vec{r},u_g'\to u_h)=\sigma_{sl}(\vec{r},u_g'\to u_h)\phi_l^m(\vec{r},u_g')\,.\tag{22}$$

The right hand side (*RHS*) of Eq. (13) can then be written as:

$$RHS=\sum_{g=0}^{G-1}\sum_{l=0}^{\infty}\sum_{m=-1}^{1}\frac{Y_{lm}^{*}(\hat{\Omega})}{4\pi}\int_{\Delta u_\perp}du_h w(u_h)\xi_i(u_h)\int_{\Delta u_\perp}du_g'\Re_{sl}^m(\vec{r},u_g'\to u_h)+\sum_{g=0}^{G-1}\frac{\chi_{ih}(\vec{r})}{4\pi k}\int_{\Delta u_\perp}du_g'\Re_f(\vec{r},u_g')\tag{23}$$

This leads us to an expansion of the incoming energy dependence of the reaction rate densities, either fission or scattering, in the chosen orthogonal basis:

$$\Re(\vec{r},u'_g)=\sum_{j=0}^{\infty}\alpha_j\Re_{jg}(\vec{r})\xi_j(u'_g) \tag{24}$$

where

$$\Re_{jg}(\vec{r})=\int_{\Delta u_\perp} du'_g\Re(\vec{r},u'_g)w(u'_g)\xi_j(u'_g)\,. \tag{25}$$

This results in the following form for the *RHS* of Eq. (13):

$$\begin{aligned}RHS=&\sum_{g=0}^{G-1}\sum_{l=0}^{\infty}\sum_{m=-1}^{1}\sum_{j=0}^{\infty}\frac{\alpha_j}{4\pi}Y_{lm}^{*}(\hat{\Omega})\int_{\Delta u_\perp}du_h w(u_h)\xi_i(u_h)\Re^m_{sljg}(\vec{r},u_h)\int_{\Delta u_\perp}du'_g\xi_j(u'_g)\\&+\sum_{g=0}^{G-1}\sum_{j=0}^{\infty}\alpha_j\frac{\chi_{ih}(\vec{r})}{4\pi k}\Re_{fjg}(\vec{r})\int_{\Delta u_\perp}du'_g\xi_j(u'_g)\end{aligned} \tag{26}$$

The form of Eq. (26) is then modified by defining the moments of the fission production cross section and the scattering kernel in the following manner:

$$\nu\sigma_{fjg}(\vec{r})=\frac{\Re_{fjg}(\vec{r})\int_{\Delta u_\perp}du'_g\xi_j(u'_g)}{\phi_{jg}(\vec{r})}\qquad\sigma^m_{sljg}(\vec{r},u_h)=\frac{\Re^m_{sljg}(\vec{r},u_h)\int_{\Delta u_\perp}du'_g\xi_j(u'_g)}{\phi^m_{ljg}(\vec{r})} \tag{27}$$

Substitute Eqs. (26) in Eq. (27) and then the resulting equation in Eq. (13) to get the general condensed form of the transport equation given in Eq. (28).

$$\begin{aligned}&\hat{\Omega}\cdot\nabla\Psi_{ih}(\vec{r},\hat{\Omega})+\sigma_{0h}(\vec{r},\hat{\Omega})\Psi_{ih}(\vec{r},\hat{\Omega})+\delta_{ih}(\vec{r},\hat{\Omega})\Psi_{0h}(\vec{r},\hat{\Omega})=\sum_{g=0}^{G-1}\sum_{l=0}^{\infty}\sum_{m=-1}^{1}\sum_{j=0}^{\infty}\frac{\alpha_j}{4\pi}Y_{lm}^{*}(\hat{\Omega})\phi^m_{ljg}(\vec{r})\sigma^m_{sljg\to h}(\vec{r})\\&+\sum_{g=0}^{G-1}\sum_{j=0}^{\infty}\alpha_j\frac{\chi_{ih}(\vec{r})}{4\pi k}\nu\sigma_{fjg}(\vec{r})\phi_{jg}(\vec{r}),\qquad h=0,1,\ldots G,\;\; i=0,1,\ldots\infty\end{aligned} \tag{28}$$

where G is the number of coarse-groups the spectrum has been divided into, and *i* represents the expansion order of the moment this equation is used to calculate.

At this point, no approximations have been made, and Eq. (28) fully describes the energy dependence of the system. By truncating the expansion after "I" terms, a solution can be found with accuracy determined only by the order of the approximation chosen.

Through this method, the energy dependence of the transport equation has been completely eliminated by folding it into the moments of the cross sections and fission distribution, and then allowing for the solution of each moment individually. This amounts to a series of $(I+1)\times G$ coupled equations which can be numerically solved for the flux moments, which can then be used to construct an approximation of the angular flux by the Eq. (29).

$$\Psi(u_h) = \sum_{i=0}^{I} \alpha_i \Psi_i \xi_i(u_h) \tag{29}$$

3.1.2 Legendre Expansion

Equation (28) was derived for an arbitrary orthogonal basis; however, for the remainder of this paper, shifted Legendre Polynomials have been chosen as the expansion basis [6]. This has several benefits that serve to greatly simplify the condensed form of the transport equation and the definitions of the cross section moments of the system. First, the weighting function, $w(u_g)$, is equal to unity, which simplifies all the moment definitions in the derivation. In addition, the definition of the cross section moments are simplified by the property of the Legendre polynomials, as well as most standard orthogonal polynomials,

$$\int_{\Delta u_\perp} du'_g \xi_i(u'_g) = \int_0^1 du'_g \bar{P}_i(u'_g) = \delta_{i0} \tag{30}$$

This relation, when applied in Eq. (27), causes the fission and scattering cross sections to vanish for all expansion orders except the 0^{th}-order, which serves to uncouple the equations in Eq. (28) such that all orders are coupled to the 0^{th}-order, but not to any others. This simultaneously increases the efficiency of the solution method and removes

the dependence of the eigenvalue and converged reaction rates on the order of the expansion.

The Legendre application of the Generalized Energy Condensation Theory can then be seen as an unfolding of the energy spectrum, as all the integral properties are encompassed in the 0th-order calculation, and the detailed shape is recovered from that solution by higher order computations. The converged eigenvalue will then be the same as the eigenvalue computed with the 0th-order approximation in Eq. (31).

$$\hat{\Omega}\cdot\nabla\Psi_{0h}(\vec{r},\hat{\Omega})+\sigma_{0h}(\vec{r},\hat{\Omega})\Psi_{0h}(\vec{r},\hat{\Omega})=\sum_{g=0}^{G-1}\sum_{l=0}^{\infty}\sum_{m=-1}^{1}\frac{Y_{lm}^{*}(\hat{\Omega})}{4\pi}\phi_{gl}^{m}(\vec{r})\sigma_{sl00g\to h}^{m}(\vec{r})+\sum_{g=0}^{G-1}\frac{\chi_{0h}(\vec{r})}{4\pi k}\nu\sigma_{fg0}(\vec{r})\phi_{g0}(\vec{r}) \quad (31)$$

Examining this approximation, as well as the definitions of the cross sections, it is apparent that the 0th-order is nothing more than the standard few-group condensation, as was desired. The perturbation term is suppressed because definition of the cross-section in Eq. (17) leads to the definition of the 0th order perturbation term in Eq. (32).

$$\delta_{0h}(\vec{r},\hat{\Omega})=\frac{\int_{\Delta u_{\perp}}du_h(\sigma(\vec{r},u,\hat{\Omega})-\sigma_{0h}(\vec{r},\hat{\Omega}))\Psi(\vec{r},\hat{\Omega},u_h)w(u_h)\xi_0(u_h)}{\int_{\Delta u_{\perp}}du_h\Psi(\vec{r},\hat{\Omega},u_h)w(u_h)\xi_0(u_h)} \quad (32)$$

This term is clearly equal to zero for any coarse group *h*.

Under the Legendre application, then, we have the following equations to solve:

$$\begin{aligned}\hat{\Omega}\cdot\nabla\Psi_{ih}(\vec{r},\hat{\Omega})+\sigma_{0h}(\vec{r},\hat{\Omega})\Psi_{ih}(\vec{r},\hat{\Omega})+\delta_{ih}(\vec{r},\hat{\Omega})\Psi_{0h}(\vec{r},\hat{\Omega})&\\ =\sum_{g=0}^{G-1}\sum_{l=0}^{\infty}\sum_{m=-1}^{1}\frac{Y_{lm}^{*}(\hat{\Omega})}{4\pi}\phi_{gl}^{m}(\vec{r})\sigma_{slig\to h}^{m}(\vec{r})+\sum_{g=0}^{G-1}\frac{\chi_{ih}(\vec{r})}{4\pi k}\nu\sigma_{fg}(\vec{r})\phi_{g}(\vec{r})&\end{aligned} \quad (33)$$

$$h=0,1,\ldots G$$
$$i=0,1,\ldots I$$

where the *j* terms have been suppressed, since all non-zero moments are eliminated by the Legendre application, and

$$\Psi_{ih}(\vec{r},\hat{\Omega}) = \int_0^1 du_h \Psi(\vec{r},\hat{\Omega},u_h)\overline{P}_i(u_h) \qquad \chi_{ih}(\vec{r},\hat{\Omega}) = \int_0^1 du_h \chi(\vec{r},\hat{\Omega},u_h)\overline{P}_i(u_h) \tag{34}$$

$$\sigma_{0h}(\vec{r},\hat{\Omega}) = \frac{\int_0^1 du_h \sigma(\vec{r},u_h)\Psi(\vec{r},\hat{\Omega},u_h)}{\int_0^1 du_h \Psi(\vec{r},\hat{\Omega},u_h)} \qquad \nu\sigma_{fg}(\vec{r}) = \frac{\int_0^1 du'_g \nu\sigma_f(\vec{r},u'_g)\phi(\vec{r},u'_g)}{\int_0^1 du'_g \phi(\vec{r},u'_g)} \tag{35}$$

$$\delta_{ih}(\vec{r},\hat{\Omega}) = \frac{\int_0^1 du_h (\sigma(\vec{r},u_h) - \sigma(\vec{r},u_h))\Psi(\vec{r},\hat{\Omega},u_h)\overline{P}_i(u_h)}{\int_0^1 du_h \Psi(\vec{r},\hat{\Omega},u_h)\overline{P}_i(u_h)} \tag{36}$$

$$\sigma^m_{slig\to h}(\vec{r}) = \frac{\int_0^1 du_h \overline{P}_i(u_h)\int_0^1 du'_g \sigma_{sl}(\vec{r},u'_g \to u_h)\phi^m_l(\vec{r},u'_g)}{\int_0^1 du'_g \phi^m_l(\vec{r},u'_g)} \tag{37}$$

With the elimination of the j^{th} moments in the description of the source term on the right side of Eq. (28), the general energy condensation method can be viewed as solving for the energy spectrum of neutrons entering group *h*. The j^{th} moment represents the neutron spectrum of the neutrons leaving various other groups to enter group *h*, which is not particularly important, as long as we know the spectrum they enter group *h* with, and this is accounted for in the i^{th} moments of the scattering kernel and fission spectrum distribution. This demonstrates the value of the decoupling. Because only the total (energy integrated) reaction rate is important in the source terms, the detailed spectrum of the flux is not needed to determine the spectrum of the source term. This allows the problem to be solved only for the 0^{th} order, and the rest of the moments to be generated from the 0^{th} order solution.

For shifted Legendre polynomials, the normalization constant of the orthogonality condition (Eq. (11)) takes the value:

$$\alpha_i = (2i+1) \tag{38}$$

and the expansion of the angular flux becomes:

$$\Psi(x,u_h) = \sum_{i=0}^{I} (2i+1)\Psi_i(x)\bar{P}_i(u_h) \tag{39}$$

3.2 Application in 1-D Discrete Ordinates

As an initial verification of the method and starting point for further development in more robust applications, the generalized condensation procedure is applied in a one-dimensional discrete ordinates formulation. Within slab geometry, Eq. (33) can be rewritten as:

$$\begin{aligned}\hat{\Omega}\cdot\nabla\Psi_{ih}(x,\hat{\Omega}) + \sigma_{0h}(x,\hat{\Omega})\Psi_{ih}(x,\hat{\Omega}) + \delta_{ih}(x,\hat{\Omega})\Psi_{0h}(x,\hat{\Omega}) \\ = \sum_{g=0}^{G-1}\sum_{l=0}^{\infty}\frac{(2l+1)P_l(\mu)}{4\pi}\phi_{gl}(x)\sigma_{slig\to h}(x) + \sum_{g=0}^{G-1}\frac{\chi_{ih}(x)}{4\pi k}\nu\sigma_{fg}(x)\phi_g(x)\end{aligned} \tag{40}$$

Here, the m subscript in the scattering term has been suppressed as it is equal to zero for slab geometry. Eq. (40) is assumed to be valid for N distinct values of the direction cosine μ, as in the standard discrete ordinates formulation of the transport equation. The scalar flux and any other angularly integrated values (such as angular current) are replaced with a Gauss-Legendre quadrature formulation [6]. The one-dimensional, discrete ordinates transport equations, with generalized lethargy collapse, are thus:

$$\begin{aligned}\mu_n\frac{\partial}{\partial x}\Psi_{ih}(x,\mu_n) + \sigma_{0h}(x,\mu_n)\Psi_{ih}(x,\mu_n) + \delta_{ih}(x,\mu_n)\Psi_{0h}(x,\mu_n) = \sum_{g=0}^{G-1}\sum_{l=0}^{\infty}\frac{(2l+1)}{2}P_l(\mu_n)\phi_{gl}(x)\sigma_{slig\to h}(x) \\ + \sum_{g=0}^{G-1}\frac{\chi_{ih}(x)}{2k}\nu\sigma_{fg}(x)\phi_g(x)\end{aligned} \tag{41}$$

$$\begin{aligned}h &= 0,1,\ldots G \\ i &= 0,1,\ldots I \\ n &= 1,2,\ldots N\end{aligned}$$

where the moments have been truncated at the I^{th} order.

In the example problems, for the sake of simplicity, we make the usual approximation of neglecting the angular dependence of the energy moment of the total cross section (both the standard and perturbation term).

CHAPTER 4

EXAMPLE PROBLEMS

As an example of the application of the generalized energy condensation theory to actual problems, several 1-D reactor problems typical of boiling water reactor (BWR) core configurations are chosen, each composed of seven fuel assemblies. The cores represent a variety of situations, including both super-critical and sub-critical systems with varying amounts of highly absorbing material (gadolinium mixed in the fuel). Each fuel assembly (see Figure 1) is based on a simplified fresh GE9 assembly design containing four regions of fuel and water mixture, each 3.2512 cm thick, surrounded by 1.1176 cm of water. In assembly 1, the two interior regions have different enrichment than the outer fuel regions. The enrichment in assembly 2 is uniform. Gadolinium is added to the two inner most regions of assembly 3 while all of the fuel regions in assembly four contain gadolinium. Appendix A contains the material definitions and densities for each material present in the system. See Figure 1 for core and assembly geometries.

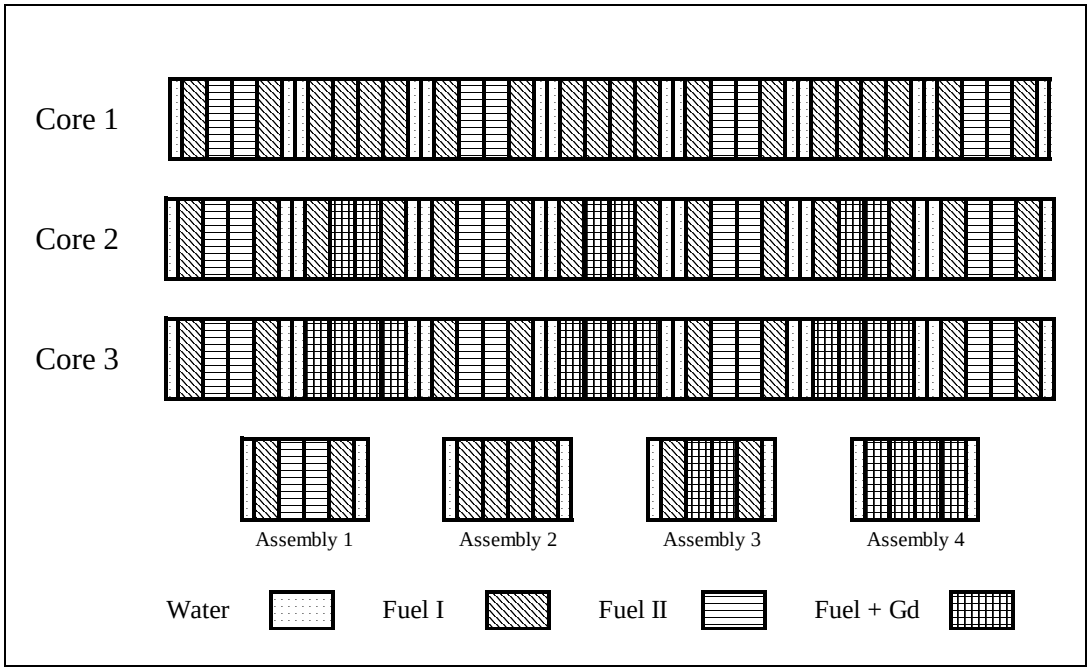

Figure 1: Sample Problem Structure

The standard discrete ordinates method using S_{16} approximation is used to calculate the individual assembly and the whole core reference solutions in 47 groups. The fine-group cross sections at the hot operating condition for each assembly were generated using the direct collision probability method in HELIOS with its 47-group production library. The single assembly 47 group solutions were used to generate the Legendre moments. The boundary conditions for the single assembly and the core calculations were specular reflective and vacuum, respectively.

Table 1 shows the eigenvalue of each assembly and core, obtained through a full 47 group transport calculation, using a one-dimensional discrete ordinates code.

Table 1: Forty-Seven Group Eigenvalues

Structure	*k*
Assembly 1	1.236117
Assembly 2	1.182026
Assembly 3	0.615100
Assembly 4	0.322272
Core 1	1.154540

Core 2	0.910321
Core 3	0.729803

Full solutions are obtained for each region of each assembly; however, for brevity, we pick several regions which are representative of the materials present in the system. The selected regions are presented in Table 2.

Table 2: Selected Regions, Assemblies

Assembly	**Region**	**Material**
1	1	Water
2	3	Fuel (Low Enrichment)
3	3	Fuel (High Enrichment)

All solutions are region-averages (over the material/layer), normalized to the total number of neutrons within the region, and integrated over all energies. Figure 2 contains the fine-group reference solution for each region in table 2.

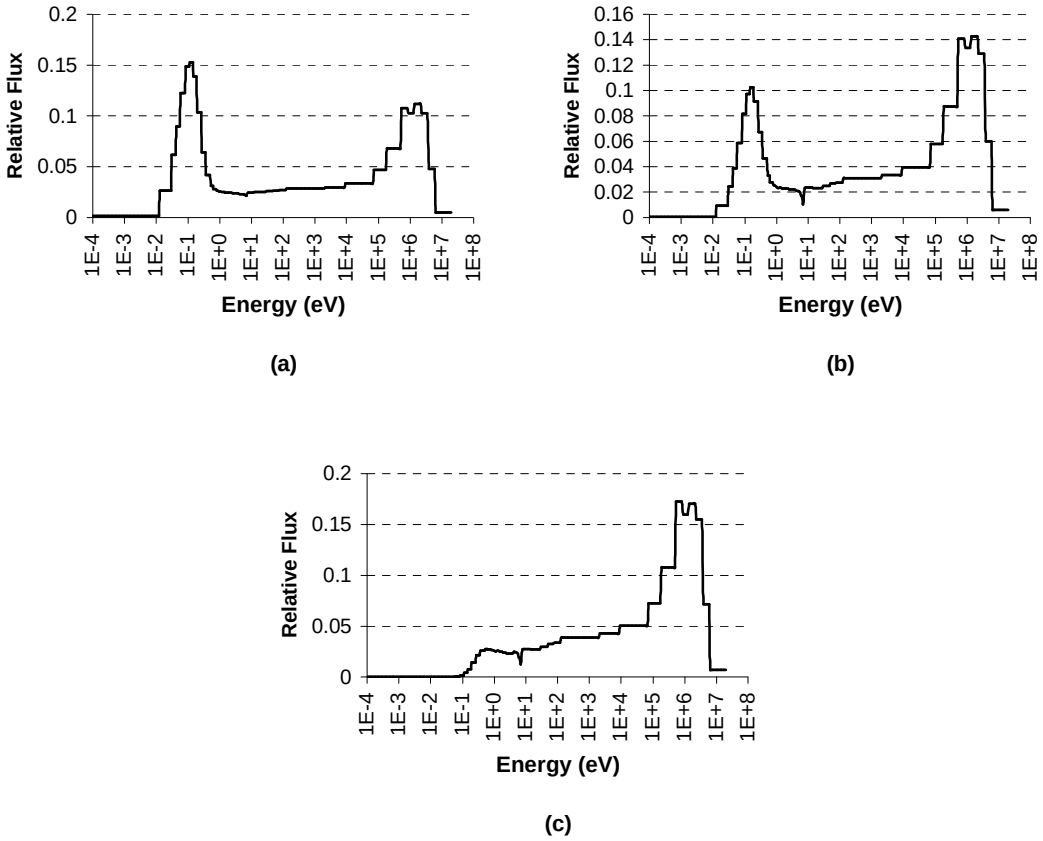

Figure 2: Fine-group Spectra (for (a) Assembly 1, Region 1 (water), (b) Assembly 2, Region 3 (fuel I), and (c) Assembly 3, Region 3 (fuel II))

4.1 Single Assembly Verification

For initial verification of the general condensation method, the 47 group flux from a fine-group transport solution performed on a single assembly is used as the weighting function during the condensation procedure. The 47 group material cross sections are condensed down to two group expansion moments of the cross sections. These are used in Eq. (41), which is used to provide an approximate solution (flux moments) for that assembly. The spectrum produced from these flux moments should, for high order, reproduce the fine group reference spectrum very accurately, since the exact solution is used as the weighting function.

For all calculations performed, in order to maintain consistency with HELIOS, transport-corrected cross sections are used. Also, as discussed earlier, the angular dependence of the total cross section is removed by weighting the fine-group transport cross section with the scalar flux as opposed to the angular flux. In addition, for the example problems, the angular dependence of the scattering kernel is treated as linearly isotropic by applying the transport correction as described below (Eq. 42). In this case Eq. (41) takes the following form.

$$\mu\frac{\partial}{\partial x}\Psi_{ih}(x,\mu)+\sigma^{tr}_{0h}(x,\mu_n)\Psi_{ih}(x,\mu_n)+\delta_{ih}(x,\mu_n)\Psi_{0h}(x,\mu_n)=\sum_{g=0}^{G-1}\frac{1}{2}\phi_g(x)\tilde{\sigma}_{sig\to h}(x)+\sum_{g=0}^{G-1}\frac{\chi_{ih}(x)}{2k}\nu\sigma_{fg}(x)\phi_g(x) \quad (42)$$

where $\sigma^{tr}_{ih}(x)$ is the moment of the transport-corrected cross section,

$$\sigma^{tr}_{0h}(x)=\frac{\int_0^1 du_h\sigma^{tr}(x,u_h)\Phi(x,u_h)\bar{P}_0(u_h)}{\int_0^1 du_h\Phi(x,u_h)\bar{P}_0(u_h)}$$

and $\tilde{\sigma}_{sig\to h}(x)$ is the energy moment of the scattering kernel, in which the within group elements have been replaced using:

$$\tilde{\sigma}_{sg\to g}(x)=\sigma^{iso}_{sg\to g}(x)-\sigma_{ag}(x)+\sigma^{tr}_{g}(x)-\sum_{h=0}^{G-1}\sigma^{iso}_{sg\to h}(x) \quad (43)$$

where $\sigma^{tr}_{g}(x)$ is the standard multigroup transport cross section. Moments of the transport-corrected scattering cross section are then condensed from the cross sections computed in Eq. (43). The perturbation moment is computed in the same manner as before, using the transport cross-section instead of the total cross section.

$$\delta(\vec{r},u)=\sigma^{tr}(\vec{r},u,\hat{\Omega})-\sigma^{tr}_{0h}(\vec{r},\hat{\Omega}) \quad (44)$$

The two-group boundary used in these examples is 0.625 eV. Standard two-group approximations (0^{th} order) for the regions in table 2 are presented in Figure 3, overlaid on the 47 group reference solution from Figure 2.

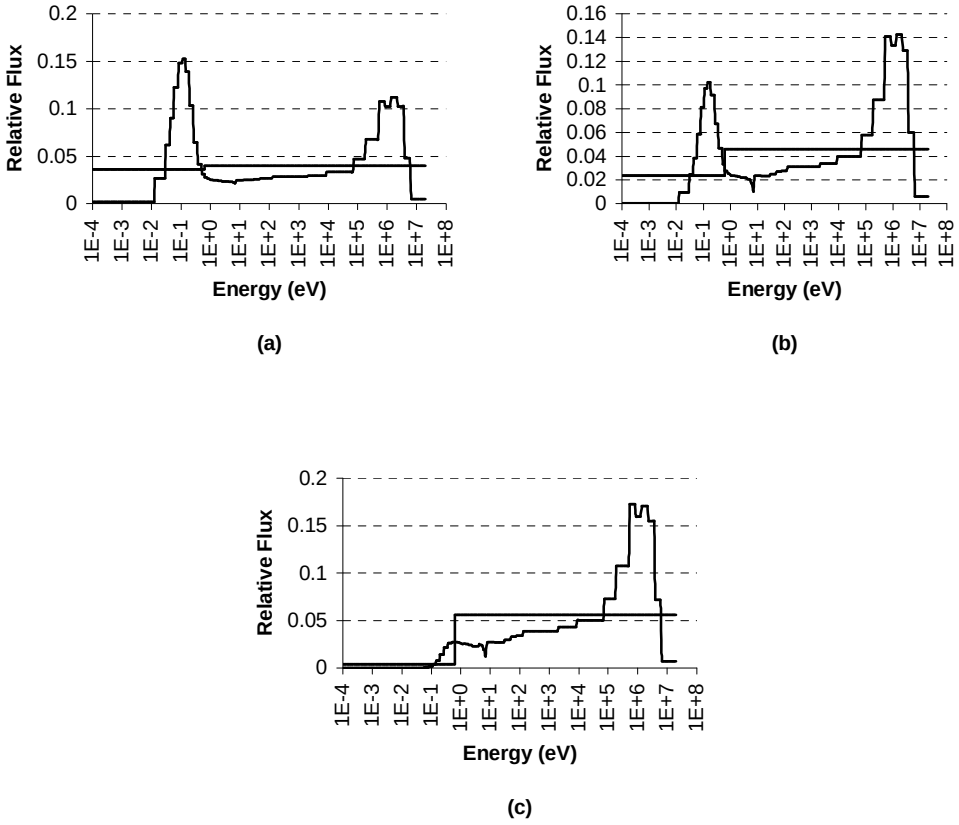

Figure 3: Standard 2-Group Collapsed Spectra (for (a) Assembly 1, Region 1 (water), (b) Assembly 2, Region 3 (fuel I), and (c) Assembly 3, Region 3 (fuel II))

Figure 3 clearly demonstrates the information loss in the condensation from many/fine-groups to a few/coarse-groups. This loss of information is quantified in the error analysis section of this paper. Next, to demonstrate the generalized condensation method, the same systems are solved using Eq. (42) for various orders of expansion *i*. As discussed previously, the eigenvalues of the expansion calculation are identical to the two-group, as a result of the properties of the Legendre polynomial set. In addition, total

fission densities and other integral properties are also completely equivalent to two group values, since preservation of the neutron reaction rates in the source distribution is strictly enforced during the condensation procedure. Due to this, if one is only interested in energy integrated quantities (such as the total fission reaction rate), than this method, in its current from, does not provide an improvement; however, Two applications are immediately apparent: shielding and detection [11,12] and reactor physics, in which one would be interested in improving the results (eigenvalue, power distributions, etc.) by re-condensation of the cross sections iteratively within the whole core calculation.

Though the eigenvalue may not improve during this initial step, the higher the order of the expansion, the more accurate the spectrum that will be produced, as is evident in Figure 4, which shows the progression from a first order approximation to a third and fifth order approximation in the fast and thermal regions of Assembly 1, Region 1 (water), overlaid with the 47 group solution.

From Figure 4, it is evident that even at low order we have spectra that are much closer to the many-group solution than the standard two-group solution. Also apparent, particularly when the flux is very near zero, is the issue of negative flux in the polynomial approximation. This is an inherent result of approximating a highly varying function with a truncated expansion, particularly when truncating at low order. This does not, however, impact the integral quantities, which are maintained in the 0^{th} term of the expansion. Presently, it is sufficient that the distribution is approaching the actual flux spectrum, with much greater detail as one goes to higher and higher order, and that negative flux values become negligible at high enough order. Figure 5 shows a twentieth order expansion approximation for the selected regions.

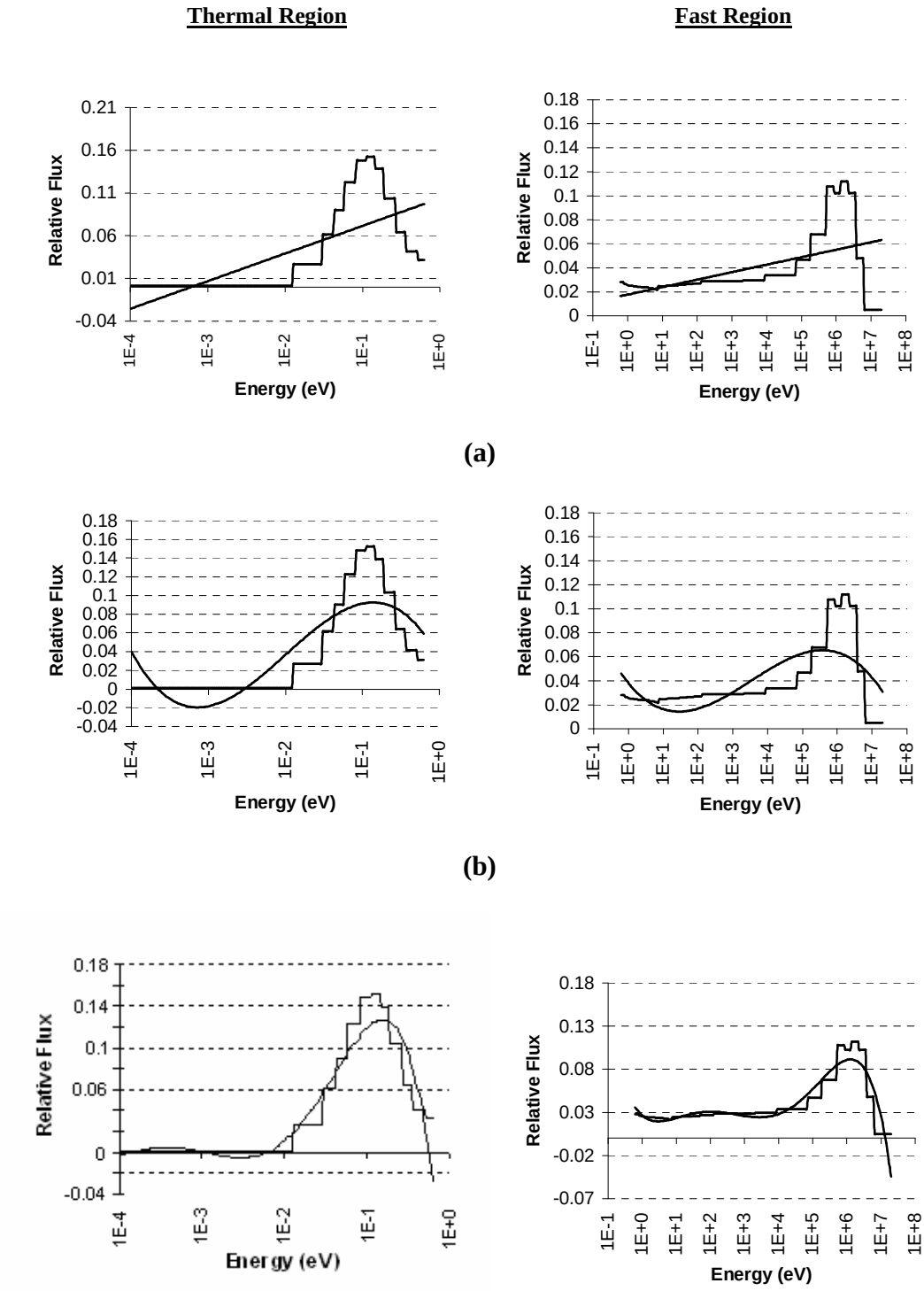

Figure 4: 1st (a), 3rd (b), and 5th (c) order approximations in Assembly 1, Region 1 (water).

Thermal Region **Fast Region**

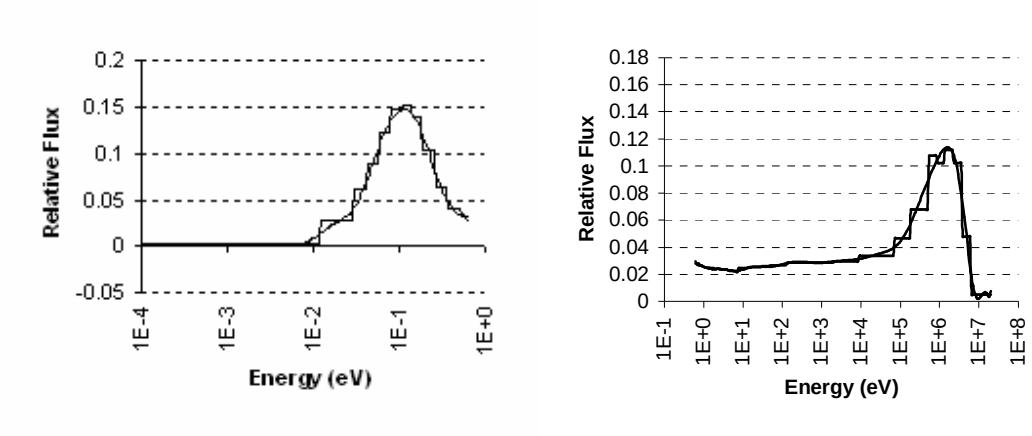

(a)

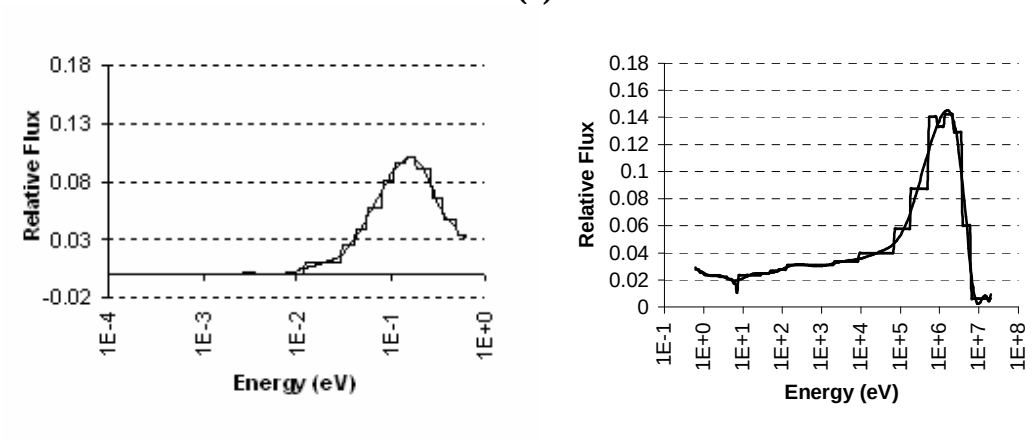

(b)

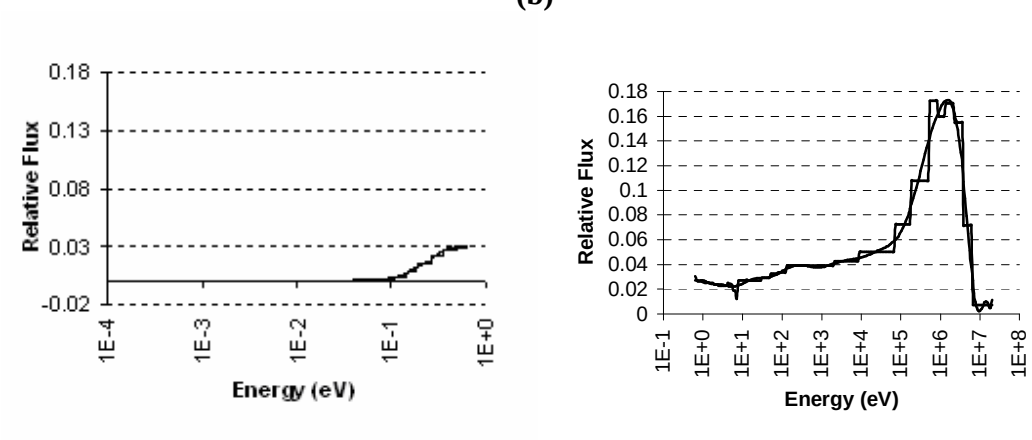

(c)

Figure 5: Twentieth Order Approximation for (a) Assembly 1, Region 1 (water), (b) Assembly 2, Region 3 (fuel I), and (c) Assembly 3, Region 3 (fuel II).

It has thus been shown that for a single assembly, using fine-group cross sections and a fine-group solution to condense the cross sections into expansion moments, a large amount of spectral information can be obtained, in contrast with standard few-group condensation methods. The solution was compared over the entire assembly, and shown to have the same accuracy as in the selected regions.

4.2 Whole Core Verification

For whole core verification, the process is as previously discussed. Single assembly, 47 group, transport calculations are performed for each unique assembly in the reactor core. The single-assembly solutions are then used to weight the fine-group cross sections for that assembly, generating region-specific, two-group, cross section moments. These moments are then used in Eq. (41) to compute two-group, core-level flux moments, which are used to produce the core-level energy spectrum of the neutron flux. As in the single assembly verification, comparisons are performed in a few representative regions. We present the results for Core 3 since this is the most heterogeneous and therefore most challenging geometry. The selected regions are shown in Table 3. Figure 6 contains the 47 group whole core reference solution, the two-group 0^{th}-order approximation for the selected core regions, as well as the twentieth order approximate solutions.

Table 3: Selected Regions, Whole Core

Core	Region	Material
3	7	Water
3	15	Fuel (High Enrichment)
3	21	Fuel + Gd

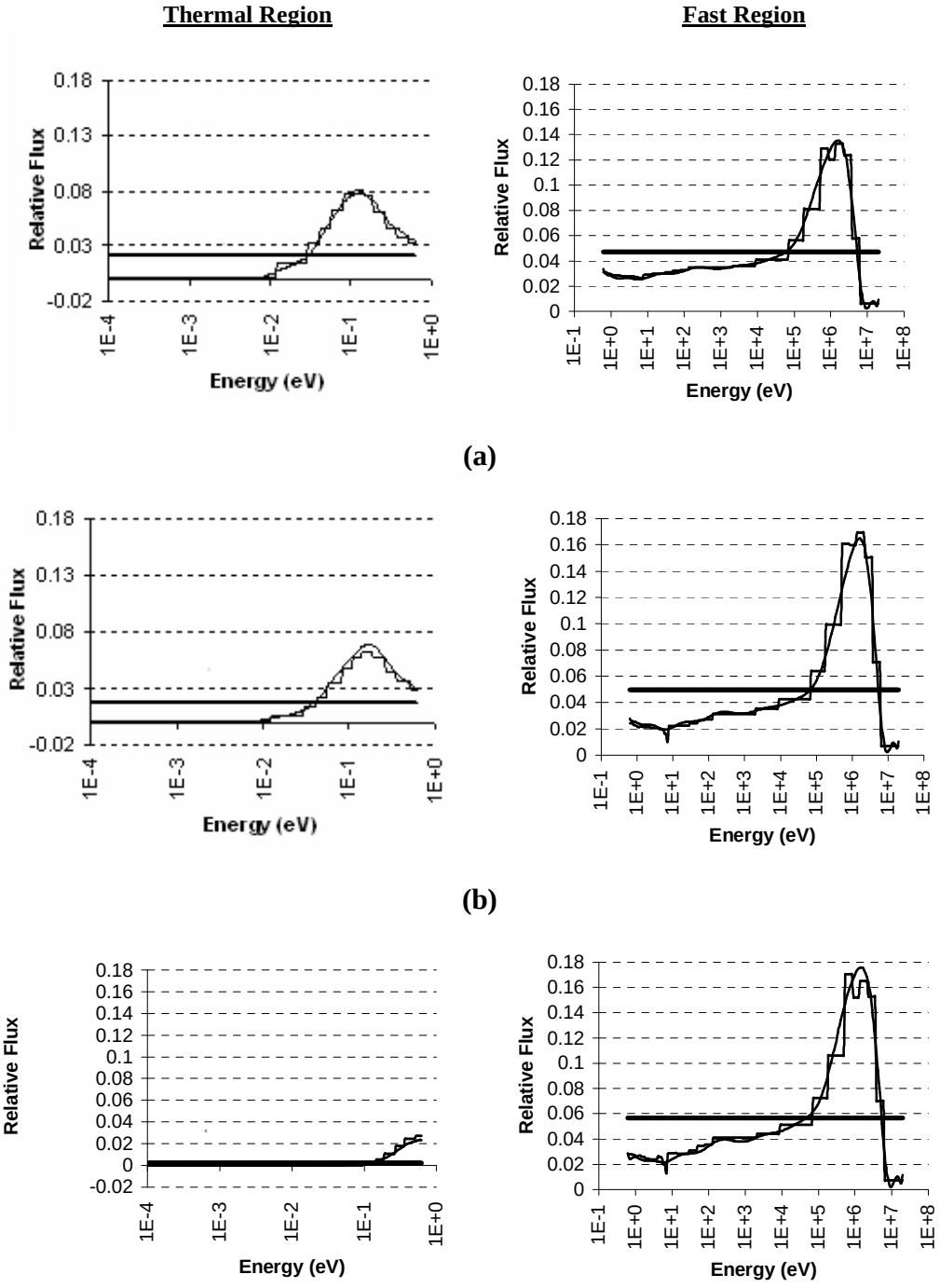

Figure 6: Core 3 Spectra ((Fine, 0^{th} order, and 20^{th} order) for regions (a) 7 (water), (b) 15 (enriched fuel), and (c) 21(fuel + gd))

The generalized method has thus produced, within each coarse-group *h*, a very accurate approximation to the energy spectrum of the neutron distribution throughout the whole core, without ever having to solve the whole core using a fine group transport solution method. Averaging over the entire core also produces figures similar to that of Figure 6, and has the same accuracy as the selected regions above.

CHAPTER 5

TIME COMPARISON AND ERROR ANALYSIS

5.1 Solution Time Comparison

The goal of the development of a generalized energy condensation theory was to produce accurate spectral information for the neutron flux during a few-group computation, with significant speedup compared to a many-group transport calculation.

As previously discussed, for certain orthogonal polynomial sets, namely those that are defined such that

$$\int_{\Delta u_\perp} du \xi_i(u) = \delta_{0i} \tag{45}$$

the computation time can be reduced even further. The selection of Legendre polynomials (and most other standard orthogonal polynomials), for instance, decouples Eq. (41) in spectral expansion order. This leaves *I* few-group equations, each coupled through the source term to the 0^{th}-order solution, as discussed in the Legendre Expansion section.

One of the advantages of this decoupling is that due to the discrete nature of the fine-group structure, the computation time for the cross section moments is dependent almost solely on the group structure chosen. Since each cross section is constant over a fine group, the only computationally expensive operation in condensation is computing the integrals of the basis function over the fine groups. These integrals depend only on the group structure (and not on the geometry or material composition), and therefore are calculated only once.

In fact, if one has already solved the problem with the standard two-group method, meaning they would already have fine-group solutions for the individual assemblies as well as the coarse-group solution for the whole core, they could produce moments of arbitrary order in negligible time, as long as they have computed the integrals of the Legendre polynomials over the fine-group energy intervals for that order. This is the greatest advantage of using basis functions that satisfy Eq. (45). In order to compare the solution times for a general case (fully coupled), rather than a simplified one (decoupled), the Legendre moments of the flux are solved as though the equations are coupled. For fair comparison, the flux moments for every order were converged to the same criteria. For all calculations presented in this paper, the flux was converged to within 10^{-4}, and the eigenvalue was converged to within 10^{-6}. "Solution Time" refers to the time it takes to solve for the flux moments. Pre-Computation is also required to generate the integrals of the basis function (Legendre Polynomials) over the energy range of each fine group. This takes approximately 2 seconds for each expansion order, when going from 47 groups to 2 groups. The pre-computation only needs to be done once, however, for each specific group structure, and from that, the cross-sections for any material specifications or geometry can be condensed for arbitrary order in negligible time (less than 3 seconds for up to 200^{th} order).

The solution time, in seconds, for convergence are presented in Table 4. These times were computed by solving the equations as though they were coupled, as would be necessary for an arbitrary set of orthogonal functions. Single assembly values are averaged over all four of the assembly types. Core values are averaged over all three core types (see Figure 1).

Table 4: Computation Times (coupled)

47g Single Assembly	19.7	47g Full Core	258.9
2g, 0^{th} Order Single Assembly	0.3	2g, 0^{th} Order Full Core	2.1
2g, 4^{th} Order Single Assembly	1.9	2g, 4^{th} Order Full Core	21.3
2g, 10^{th} Order Single Assembly	6.3	2g, 10^{th} Order Full Core	69.2

Table 4 does not take advantage of the decoupling of spectral moments, and therefore the times produced are characteristic of those that would appear for any choice of basis function. Even without the decoupling, the improvement in computation time it is evident from Table 4, which shows a significant speedup for the 10^{th} order. As will be seen later (figure 8), the 10^{th} order full core solution is off by less than 3% RMS. This is because performing a 10^{th}-order calculation, without decoupling, requires the solution of 22 equations (11 expansion orders * 2 coarse-groups), whereas solving with the fine-group method requires the solution of 47 equations.

The standard two-group method gives one the ability to solve the system in approximately 0.7 - 1.5 % of the time it takes to solve the fine-group, however, one loses detailed spectral information. The new method, in its coupled form, however, produces that information, and still only requires (for 10^{th}-order) about 30% of the computation time of the fine-group calculation. For large reactors or highly complex shielding problems which can take hours or days to solve, this can reduce the needed time by a significant amount. In this manner, the new method, even without decoupling, is faster than performing fine-group, whole-core transport calculations.

The use of Legendre Polynomials, as discussed earlier, decouples the spectral moments in the right hand side of Eq. (41), which greatly speeds up the solution. When taking advantage of the decoupling of the spectral moments by solving the system in the

0^{th}-order, and then unfolding the spectral dependence from that solution, the computation times reduce significantly, as seen in Table 5.

Table 5: Solution Times for Legendre Polynomials (decoupled)

47g Single Assembly	19.7	47g Full Core	258.9
2g, 0^{th} Order Single Assembly	0.25	2g, 0^{th} Order Full Core	2.1
2g, 4^{th} Order Single Assembly	0.33	2g, 4^{th} Order Full Core	2.2
2g, 10^{th} Order Single Assembly	0.33	2g, 10^{th} Order Full Core	2.3

In this manner, the Legendre generalized equations are solved in a time comparable to that of the standard two-group solution (0.7 – 1.5 % of the fine-group computation time), but with a large amount of spectral information produced. Each additional order adds the computational time of a single outer iteration, which is negligible given the number of inner iterations performed in the core calculation.

5.2 Error Analysis

We have shown that the generalized condensation theory does an effective job of preserving the fine group spectrum during a coarse group whole core transport solution. It remains however, to quantify the improvement this allows over standard two group solutions. The total flux in each coarse group, which is the most important quantity, has been preserved by the method, but if one wants to unfold the spectrum and determine an approximate whole core flux for a subinterval of the coarse group, such as to compare detector response, there is no readily available technique for use in neutron transport problems. It is here that the generalized condensation theory becomes very useful.

To demonstrate, a solution was obtained for several systems using generalized expansion theory. This solution was then integrated over the fine-group limits, and the RMS error from a fine-group transport solution was computed for several orders of expansion. The first system tested in this manner was a simple, homogeneous 1-D slab

composed of the enriched fuel material used in Assembly 2 in the previous section, with specular reflective conditions on both sides. A 47-group solution was obtained, and this solution was used to generate 2-group moments. The expansion equations (Eq. 40) were then solved for a series of increasing orders. From this, the reconstructed 47-group flux was computed by integrating the flux over the fine-group limits. How close the47 group flux is to the reconstructed flux is a good measure of how effectively the high order effects are preserved. The RMS error of these group fluxes, as a function of expansion order are plotted in figure 7. As seen in figure 7, the flat flux (0^{th} order) has an RMS error of 23.9%. It is also clear from figure 7 that for high expansion order, the expanded flux is approaching the fine-group flux.

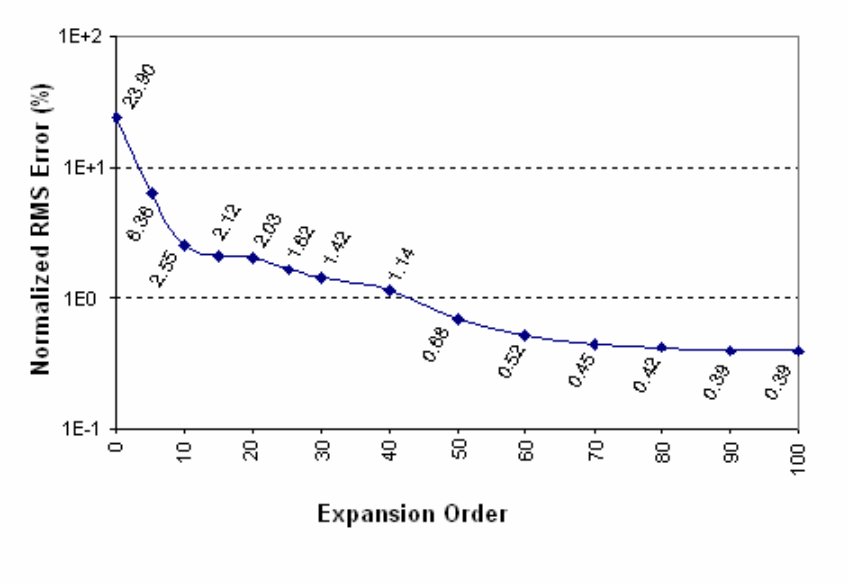

Figure 7: Group Flux Error vs. Expansion Order for a Homogeneous Slab

Figure 7 demonstrates that the generalized condensation theory is able to produce the fine-group spectrum quite well. It does not, however, demonstrate how this will affect whole-core problems when the assembly level flux is used to condense, as is the case in practical application.

One of the most useful aspects of the generalized theory is that it results in a solution that is much closer to the core level reference than to the assembly level flux that was used to weight the moments. To show how effective the generalized method is in producing the core-level spectrum, the same computations were done as in the homogenous slab, averaged over the entirety of core 3. The expansion solution was computed for a series of orders, as in the slab problem, and the resultant group flux was compared with the whole-core fine-group reference solution. These results are presented in figure 8.

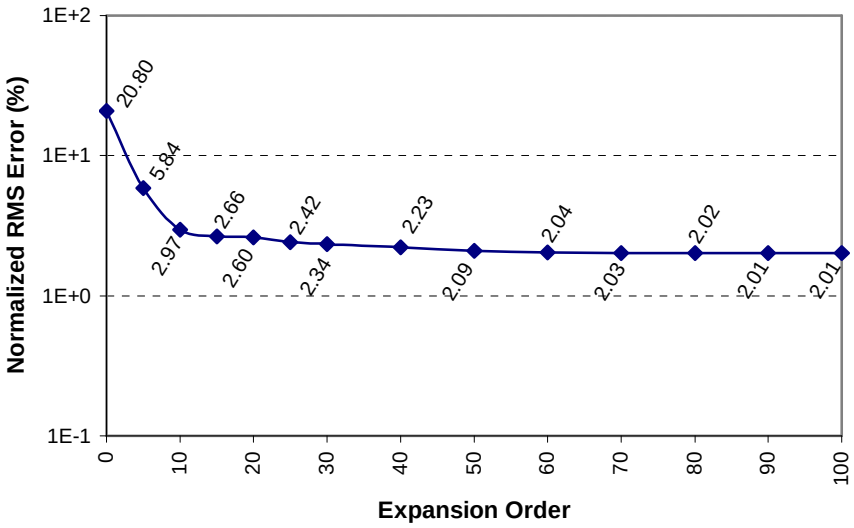

Figure 8: Group Flux Error vs. Expansion Order for Core 3.

As is evident in figure 8, the expansion solution converges to about 2% away from the core-level reference solution (RMS). The expansion solution is, by comparison, 15.3% away from the assembly-level, fine-group transport solution. The expansion solution on the core-level is therefore significantly closer to the actual core-level flux, even at relatively low order. This implies that an iterative condensation procedure has merit (see the summary and future work section).

CHAPTER 6

CONCLUSIONS AND FUTURE WORK

The standard multigroup theory has been generalized in this paper. The new energy condensation theory generates detailed (many-group) spectral resolution within the few-group structure without the computational expense associated with solving the many-group transport equations. The generalization, which contains the standard multigroup theory as a special (0^{th}-order) case, is achieved by using an energy expansion of the angular flux in an arbitrary set of orthogonal functions. This expansion leads to a set of equations for the energy moments of the flux with a coupling characteristic that directly depends on the choice of the expansion functions. It was shown that the higher moment equations are only coupled to the 0^{th}-order moment equation and not to each other if Legendre polynomials are used as the expansion set. As a result of this decoupling, the computational time associated with the solution of the higher order moments become negligible as compared to that for the 0^{th}-order solution. This desirable feature makes the new theory very attractive for application to reactor core simulations since the few-group calculations can now produce the energy resolution of the many-group method with negligible computational penalty. The method was developed in the framework of transport theory. However, its extension to diffusion theory is straightforward.

The new theory, which is completely independent of the transport solution method, was verified and tested in a few 1-D BWR benchmark problems within the discrete ordinates approximation. As expected, it was shown that the energy resolution

within a two-group structure is increased with increasing expansion order close to that of the reference (47) fine-group spectrum with computational expense competitive to that of the standard two-group solution.

One of the issues with condensation is that the data we have to input into the problem is discrete, and anytime a continuous expansion basis is being used to approximate a discrete set of points, numerical issues arise, such as Gibbs oscillations at energy group boundaries. These are mostly small effects, but in cases where it is desirable to remove such effects, one possible way to correct this issue is to implement a discrete form of Legendre Polynomials [10]. The method presented in this paper (with continuous Legendre Polynomials) can already produce the fine-group spectrum to a high degree of accuracy, but because they do not suffer these numerical effects, using discrete Legendre Polynomials could possibly produce the same results more efficiently. Discrete Legendre polynomials might make it possible to produce high accuracy solutions at lower orders, and cut down on pre-computation time.

We note that the generalized method is not limited to reactor eigenvalue problems as applied in this paper. This in general is an energy unfolding method and therefore should find applications to detection and shielding problems as future work.

The most common use of spectral unfolding similar to this method is in detection, either for neutrons, photons, or electrons. One problem inherent in detection schemes is the inherent imperfections of spectrometers. Detector responses must be passed through an unfolding scheme to determine actual incident neutron spectra. This is due to the individual detector mechanics causing the incidence of neutrons at various energies to bin themselves into a discrete number of channels. The standard method (FERDoR

technique) for unfolding requires knowledge of the particular folding effect of that individual detector, in order to invert that effect. [11,12] This can be done in a couple of ways; however, the generalized method can potentially provide a way to determine it more exactly, by using a transport or Monte Carlo solution and folding it into the appropriate bins for that scenario. Then, within each bin, the actual spectrum can be unfolded based on the detector response. These applications will be tested as future work.

Given that the whole-core expansion solution produced a result significantly closer to the fine-group whole-core transport solution than to the fine-group assembly-level solution, it would be very useful and interesting to extend the method to re-condense (update) the fine-group cross sections within the few-group calculations in a self contained iterative manner. In this way, the few-group macro or microscopic cross sections are corrected for spectral effects and as a result one would expect significant increase in accuracy of the few-group calculations with negligibly small additional computational effort. As seen in the example problems, slightly negative fluxes may result in some energy ranges because of the flux expansion. It is not clear if these negative fluxes would present a problem with the re-collapsing procedure.

APPENDIX A

BENCHMARK PROBLEM MATERIAL DEFINITIONS

Region dependent macroscopic cross sections for the benchmark problems were generated using the HELIOS[8] collision probability lattice depletion code. The 47 group production library based on the ENDF/B-VI.8 data files [7, 8] was used as the fine-group library. The compositions of the materials used in the assemblies are given in Table A-1.

Table 6: Material Definitions, Densities in $10^{24}/cm^3$

Material	**Component**	**Number Density**
Water	^{16}O	2.02E-2
	^{1}H	4.03E-2
	Natural Zr	7.86E-3
Fuel 1	^{234}U	1.50E-6
	^{235}U	1.68E-4
	^{238}U	7.39E-3
	^{16}O	2.87E-2
	^{1}H	2.73E-2
	Natural Zr	4.79E-3
Fuel 2	^{234}U	2.52E-6
	^{235}U	2.75E-4
	^{238}U	7.28E-3
	^{16}O	2.87E-2
	^{1}H	2.73E-2
	Natural Zr	4.79E-3
Fuel + Gd	^{234}U	2.63E-6
	^{235}U	2.87E-4
	^{238}U	6.88E-3
	^{16}O	2.86E-2
	^{1}H	2.73E-2
	Natural Zr	4.79E-3
	^{154}Gd	9.68E-6
	^{155}Gd	6.58E-5
	^{156}Gd	9.10E-5
	^{157}Gd	6.96E-5
	^{158}Gd	1.10E-4
	^{160}Gd	9.80E-5

These 1-D material compositions (isotopic densities) were derived by approximately conserving the transverse integrated reaction rates of the 2-D GE9

assembly design of reference [9]. For the computation of the macroscopic cross sections using HELIOS, it was assumed that the assembly was at the hot operating condition; i.e., 833K for fuel and 500K for coolant/moderator.

REFERENCES

[1] M.L. Williams and M. Asgari, "Computation of Continuous-Energy Neutron Spectra with Discrete Ordinates Transport Theory", *Nuclear Science and Engineering.* **121**, 173-201 (1995)

[2] M.L. Zerkle, "Theory and Application of Deterministic, Multidimensional, Pointwise Energy Lattice Physics Methods," *B-T-3287*, Bettis Atomic Power Library (1999).

[3] M. L. Zerkle, I. K. Abu-Shumays, M. W. Ott, and J. P. Winwood "Theory and Application of the RAZOR Two-Dimensional Continuous Energy Lattice Physics Code," *Proceeding of the Joint International Conference on Mathematical Methods and Supercomputing for Nuclear Applications*, Saratoga Springs, New York, October 5-9, 1997, Vol. 1, pp. 417-428, American Nuclear Society (1997).

[4] M.L. Williams, "Pointwise Energy Solution of the Boltzmann Transport Equation for Thermal Neutrons," DOE/ID/13765, (2001)5. R. N. Silver, H. Roeder, A. F. Voter and J. D. Kress, "Kernel Polynomial Approximations for Densities of States and Spectral Functions," *J. Comput. Phys.* **124**, 115-130 (1996).

[6] Lewis, E.E. and Miller, W.F., Jr. (1993), "Computational Methods of Neutron Transport, *American Nuclear Society*, La Grange Park, Illinois.

[7] P. F. Rose and C. L. Dunford, Eds., "*ENDF-102, Data Formats and Procedures for the Evaluated Nuclear Data File, ENDF-6*," Brookhaven National Laboratory report BNL-NCS-44945 (July 1990).

[8] Giust, F.D. (2000), Release Notes for Helios System 1.6, *Studsvik Scandpower Report*, SSP-00/205, January 03.

[9] D.J. Kelly, "Depletion of a BWR Lattice Using the RACER Continuous Energy Monte Carlo Code," *Proceedings of the International Conference on Mathematics and Computations, Reactor Physics and Environmental Analyses*, Portland, Oregon, April 30-May 4, Vol. 2, p. 1011, American Nuclear Society (1995).

[10] S.W. Mosher, "A Variation Transport Theory Method for Two-Dimensional Reactor Core Calculations," Ph.D. Thesis, Georgia Institute of Technology, June 2004.

[11] W.R. Burris, V.V. Verbinski, "Fast-Neutron Spectroscopy with Thick Organic Scintillators," ORNL – TM – 2225, June 25, 1968.

[12] W.R. Burris, "Utilization of A Priori Information by Means of Mathematical

Programming in the Statistical Interpretation of Measured Distributions," Ph.D. Dissertation, Ohio State University, June 1965. (ORNL-3743)